

Appendix F

ANALYSIS FROM AVAILABLE TECHNICAL INFORMATION ON PIPELINE RUPTURE

By Dr. Robert E. Nickell

Introduction

The preparation of this appendix was a consequence of the Panel's deliberation process. Originally, the Panel's technical consultants were instructed to monitor the progress of the NTSB investigation of the San Bruno failure, using the Board's preliminary findings on potential contributing factors as the basis for assisting the Panel in framing its conclusions and recommendations. However, after reviewing the NTSB staff metallurgical results, reviewing the recollections and observations of the NTSB interviewees, and actually visiting the site of the incident with an opportunity to directly discuss those observations with some of the NTSB interviewees, the technical consultants determined the framework to be presented to the Panel was sufficiently complex to require formal articulation. The logical flow of that framework is provided in the following.

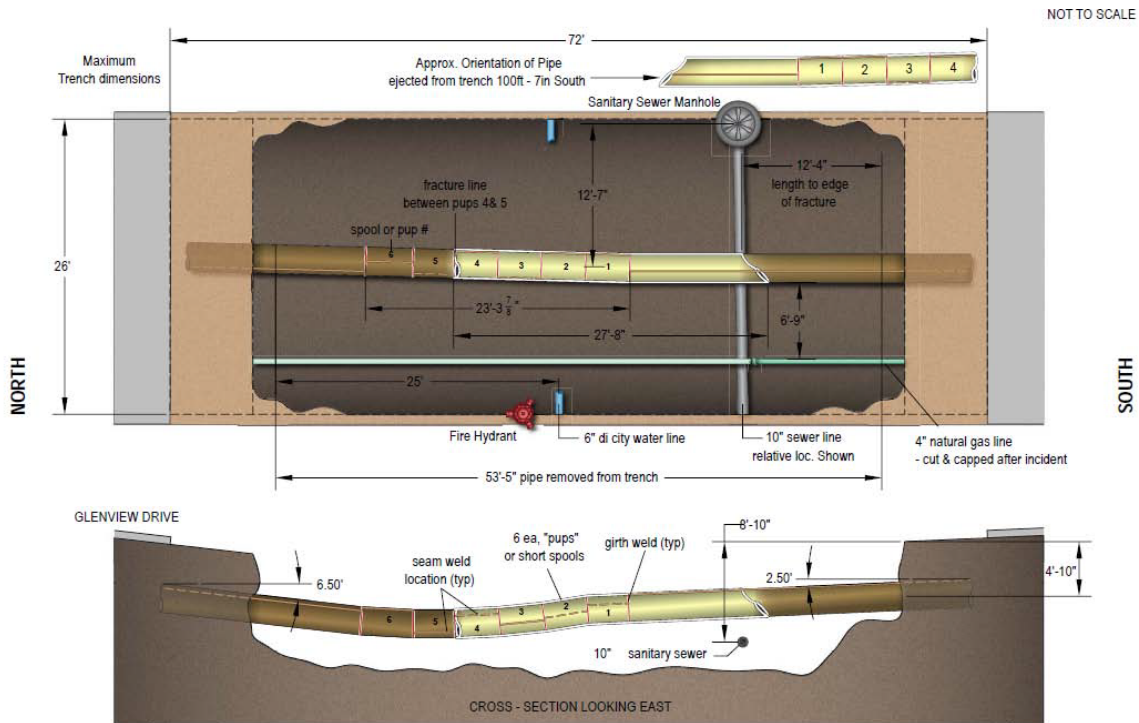
The Pipeline Geometry and Terrain Topography

The pipeline geometry and associated terrain topography are illustrated in the sketch of the segment used by the NTSB as a reference for their March 2011 hearings, as shown in Figure F-1 below. This figure shows both a plan view (on top) and an elevation view (on the bottom) that illustrates the relative location of the affected portion of the pipeline, the surrounding topography, and other relevant features such as the number of piping sections (referred to as PUPs) that were circumferentially welded together to form the total segment crossing the ravine on fill. From the figure, a relatively long piping run extends from the south end of the ravine and connects to PUP 1 at a point about 40% of the distance across the ravine and some ten feet or so north of the point where the June 2008 San Bruno city sewer replacement lateral crosses under the 30-inch-diameter, 0.375-inch-wall-thickness gas transmission line. PUP 1 connects to PUP 2 and then to PUP 3, and so on, until a final connection between PUP 6 and a relatively long piping run that extends out of the fill region into the north end of the ravine.

Two observations come to mind from the figure. First, the decision to place such a circumferential-weld-connected system of short piping runs together in a ravine fill section would normally trigger concerns about threats due to earth movement and possibly to the effects of water pressure during heavy rains. This concern would be amplified by knowledge about the location and orientation of the pipeline relative to seismic activity along the Daly City-Serramonte-San Bruno axis, with potential for lateral motion and soil liquefaction. Second, knowing the location of PUP 1 relative to the lateral crossing of the San Bruno city sewer lateral,

even if the seam weld defect was not known, should have triggered a significant concern during any excavation and related disturbances during the sewer replacement project in June 2008.

Figure F-1 Schematic of the failed pipeline segment in both plan and elevation view¹



Very little information is available from fabrication and installation records for the placement of this pipeline segment in 1956, and the little amount of information tends to be anecdotal. For example, Exhibit No. 2-F, Docket No. SA-534 (the Maffei interview) provides anecdotal information about the problems encountered with fit-up of piping segments, because of the terrain, during the 1956 installation, resulting in considerable torch cutting of the piping segment ends to prepare circumferential weld joints. It seems likely the short PUP segments were introduced in order to minimize girth weld joint preparation, with the possibility that short piping segments with uncertain or unknown pedigree were located and used. Maffei also describes the visual examination he performed on approximately 1700 feet of the Line 132 piping run, crawling on his hands and knees through the 30-inch-diameter line. He was not looking up nor was he looking laterally to observe any potential defects in the longitudinal seam welds, being

¹ Preliminary Analysis of Publicly Available Evidence Supporting a Failure Cause of the PG&E San Bruno Incident, INGAA Pipeline Safety Committee, May 5, 2011, Interstate Natural Gas Association of America, Washington, DC.

much more concerned with crawling across the protruding girth welds, where his knees could receive some degree of injury.

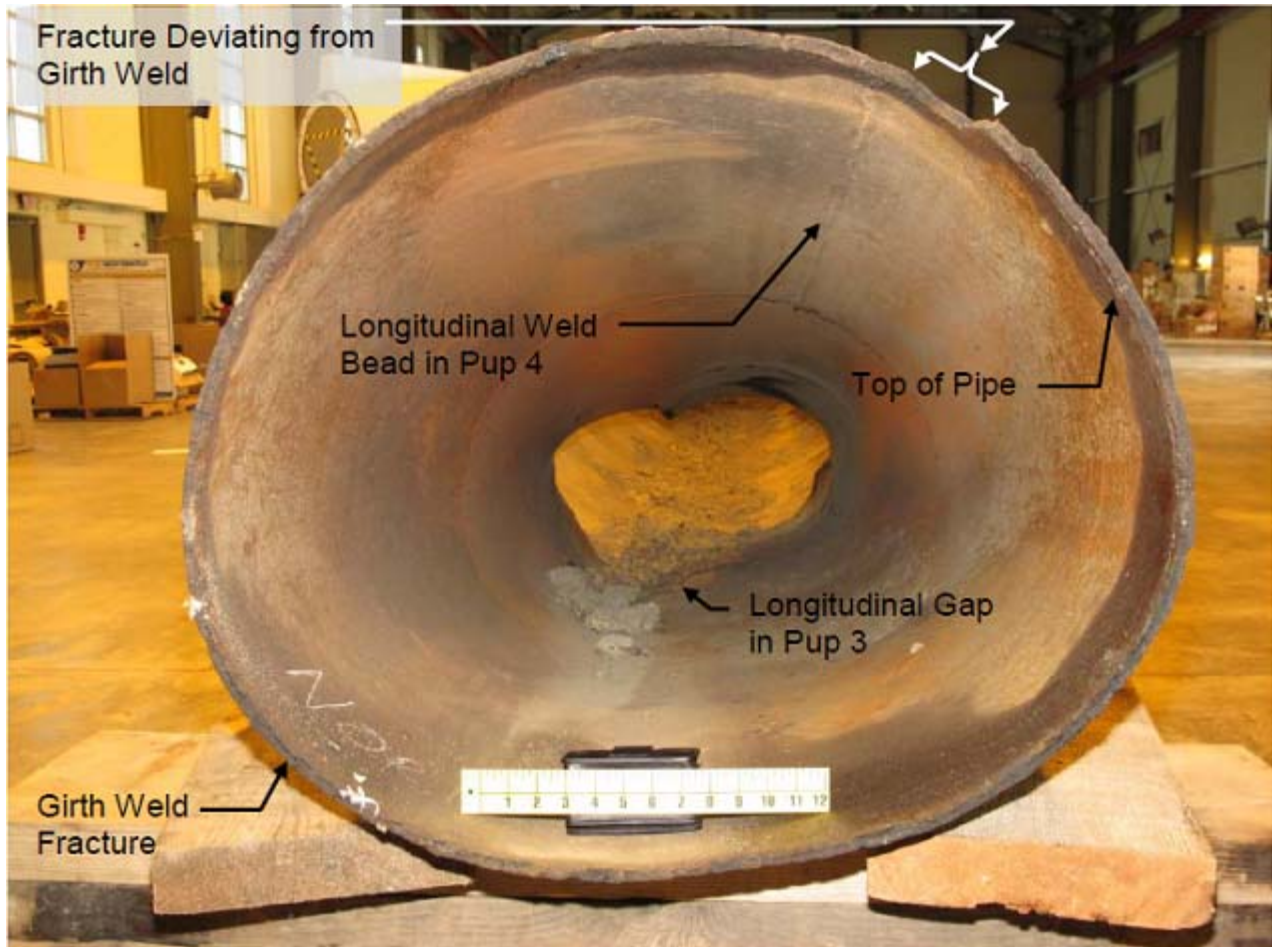
To confirm the Maffei statements, Table F1 (see below) of NTSB Metallurgical Report 1 (Report No. 10-119) provides the orientation of the longitudinal weld seams in the various pieces of pipe that constitute the failed San Bruno pipeline segments, as measured in the NTSB laboratory. The distances are given in inches measured circumferentially – clockwise or counterclockwise – from the top of the pipe looking North. In order to grasp the angular significance of those circumferential measurements, it should be noted the total circumference is greater than 90 inches. From the table it can be seen that, for the long joint South of PUP 1, the longitudinal weld seam is almost directly at the top of the pipe, only 2.88 inches clockwise from the top of the pipe. For PUP 1, the longitudinal seam fracture is located on the East side of that piece, roughly at 70 degrees from the top of the pipe. For PUP 2, the longitudinal seam fracture is also on the East side of that piece, almost at 90 degrees from the top of the pipe.

A good check on the longitudinal seam orientations is provided by Figure F2 from Report 10-119, which shows the longitudinal seam weld in PUP 4 looking South. The 15.25-inch clockwise measurement given in the table (about 58 degrees from the top of the pipe) can be directly compared to the angular location of the longitudinal weld bead shown in Figure F2, which appears to be a little more than 45 degrees counterclockwise (looking South) from the top of the pipe.

Table F1: Circumferential Distance of Longitudinal Seams and Longitudinal Fractures Measured from the Top of the Pipe

Pipe Piece / Feature	Circumferential Distance from Top of Pipe, inch
Long Joint South of PUP 1 – DSAW Seam	2.88 inch – Clockwise
PUP 1 – Longitudinal Fracture	18.50 inch – Clockwise
PUP 2 – Longitudinal Fracture	24.75 inch – Clockwise
PUP 3 – Longitudinal Fracture	27.25 inch – Counterclockwise
PUP 4 – Longitudinal Fracture	15.25 inch – Clockwise
PUP 5 – Longitudinal Fracture	34.25 inch – Counterclockwise
PUP 6 – Longitudinal Fracture	0.38 inch – Counterclockwise
Long Joint North of PUP 6 – DSAW Seam	11.50 inch – Counterclockwise

Figure F-2: Fracture Through the Girth Weld Between PUP 4 and PUP 5 at the North End of the Center Section. The View is Looking South. PUP 3 and PUP 2 are Also Visible.



From the table and the figure, two features can be observed: (1) some attempt was made during installation to offset longitudinal weld seams from one piping segment to the next; and (2) most, but not all, of the longitudinal weld seams were located in the top portion of the pipe segments. With particular regard to the PUP 1 and PUP 2 segments, the location of the longitudinal weld seams are both fairly close to 90 degrees from the top of the pipe segments on the east side of the pipe run. This implies large, unbalanced pressure loads on the east side of the pipe run, such as could be caused by completely backfilling the east side after excavation, without corresponding backfill on the west side, would cause “flattening” on that side of both segments, placing the inside of the pipe segments at those locations (and the deepest portions of any internal defects) in tension.

Mechanical Properties

Chemical and mechanical property measurements for the removed San Bruno pipe segments were given in NTSB Metallurgical Report No. 2 also referred to as Report No. 11-005. Both sets of measurements showed consistent and anomalous behavior for several of the segments – notably PUP 2 – but also, to a lesser extent, PUP 1, PUP 3, and PUP 5. In order to discuss these anomalies, the first two data columns of the chemistry Table F2 have been extracted (see below), along with Tables F2A1 (yield strength), F2A2 (ultimate tensile strength), and F2A3 (total elongation).

Table F2 from 11-005. Chemistry Data for San Bruno Piping Segments

Sample	C	Mn
LS	0.29	1.02
P1	0.24	0.34
P2	0.12	0.35
P3	0.21	0.32
P4	0.18	0.8
P5	0.28	0.62
P6	0.27	0.95
LN	0.2	1.02
RW	0.1	0.49

The most startling anomaly is the combined low carbon content (0.12%) and the low manganese content (0.35%) for the chemistry of PUP 2, when compared to the API 5LX X42 specification of 0.33% and 1.28%, respectively, for carbon and manganese. Since these two alloying elements are largely responsible for the steel strength, it is not surprising the yield strength for all five mechanical property samples taken from PUP 2 gave very low yield strengths. It is also worth noting that, for the pipe segments with nominal carbon and manganese in the correct range (see both the long south segment adjacent to PUP 1 and the

long north segment adjacent to PUP 6), the yield and ultimate tensile strengths are quite acceptable without compromising the ductility (elongation). It is also worth noting the chemistry of the piece of welding rod (WR) that was found embedded in one of the pipe segments during the investigation is also unsatisfactory, which does not bode well for the girth welds.

Potential decarburization during service seems to be an unlikely explanation, since no other significant evidence of corrosion was found during the investigation. The poor strength of the PUP 1, PUP 2, PUP 3, and PUP 5 segments appears to be due to either low carbon or low manganese, or a combination of both. Whether such anomalous chemistry and strength is systemic throughout the 150 miles of uncharacterized legacy gas transmission piping in the PG&E system is unknown.

Table F2A1: Yield Strength Data Using the 0.5% Extension Under Load Method for Each Tensile Test Specimen

Source	Test 1, ksi	Test 2, ksi	Test 3, ksi	Test 4, ksi	Test 5, ksi
LS	56.0	57.0	57.0	57.5	57.5
P1	36.9	36.3	36.8	36.6	36.3
P2	32.1	32.0	31.9	32.0	32.1
P3	35.3	34.9	34.1	34.9	35.3
P4	47.7	49.1	47.9	48.3	48.4
P5	38.9	38.4	38.6	38.6	38.2
P6	48.5	51.5	50.5	50.0	52.0
LN	54.0	54.5	53.5	54.0	54.0

Table F2A2: Tensile Strength Data for Each Tensile Test Specimen

Source	Test 1, ksi	Test 2, ksi	Test 3, ksi	Test 4, ksi	Test 5, ksi
LS	83.5	83.0	83.0	83.0	83.5
P1	63.5	63.5	64.0	63.5	63.5
P2	52.0	52.0	52.0	52.0	52.0
P3	60.5	60.5	60.0	60.0	60.5
P4	79.0	79.0	79.0	79.0	79.0
P5	72.0	72.0	72.0	71.5	71.5
P6	78.5	78.5	79.0	79.0	78.5
LN	76.5	77.0	77.0	77.0	77.0

Table F2A3: Total Elongation for Each Tensile Test Specimen

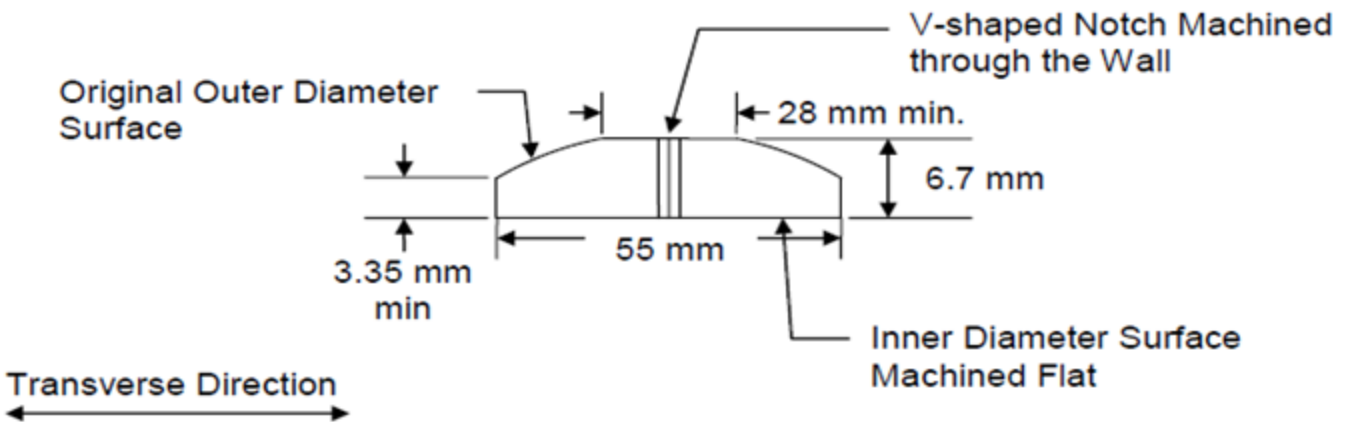
Source	Elongation, % in 2 inch				
LS	30	31	30	29	30
P1	39	39	40	39	40
P2	49	48	48	50	49
P3	42	43	43	43	43
P4	33	34	34	34	35
P5	34	36	36	37	36
P6	31	31	30	30	32
LN	31	31	30	30	30

NTSB metallurgical report 11-005 also provided information on the impact energies of the base metal in the various Line 132 piping segments, which can be used to estimate the fracture toughness properties. The data are taken from Table A5, extracted and shown below. The samples used for Charpy impact testing were slightly sub-size, as shown in Figure F3 from 11-005, extracted and shown below.

Table F2A5: Impact Toughness Values for Each Charpy Test Specimen

Source	Test 1, ft-lbs	Test 2, ft-lbs	Test 3, ft-lbs	Test 4, ft-lbs	Test 5, ft-lbs	Test 6, ft-lbs
LS	10.0	11.0	10.0	10.0	11.0	10.0
P1	9.0	6.0	7.0	6.0	6.0	8.0
P2	76.0	25.0	99.0	52.0	27.0	18.0
P3	8.0	8.0	8.0	9.0	9.0	8.0
P4	13.0	10.0	12.0	11.0	11.0	14.0
P5	14.0	7.0	7.0	6.0	7.0	9.0
P6	10.0	11.8	8.0	8.0	10.0	10.0
LN	16.0	14.0	15.0	11.0	11.0	9.0

**Figure F3: Schematic of Charpy Impact Test Specimens Taken from Each Piece of Pipe
The Longitudinal Axis of the Pipe Runs In and Out of the Page**



Note LS and LN denote data for the south and north long pipe segments attached to PUP 6 and PUP 1, respectively. P1 through P6 denote data for the PUP piping sections. All of the specimens were taken from base metal and none of the data are for weld or heat-affected zone material. The impact data for PUP 1 (P1) show a variation from 6.0 to 9.0 ft-lb. The specimens are only slightly sub-size, since the full 10 mm dimension was available along the pipe axis, and 6.7 mm out of 10 mm was available through the pipe wall thickness (see Figure 3 from NTSB 11-005).

Various correlations can be used to scale the 6 ft-lb to 9 ft-lb sub-size Charpy data to full scale, and then to estimate the fracture toughness, with results that vary from as low as 35 ksi $\sqrt{\text{in}}$ up to perhaps 45 ksi $\sqrt{\text{in}}$. The precise value is not as important as the knowledge that the fracture toughness is relatively low in comparison to the value that would normally be expected for typical piping base metal. It would be expected the fracture toughness of the weld and heat-affected zone would be lower, but perhaps not very much lower.

Initial Manufacturing Defect Assessment

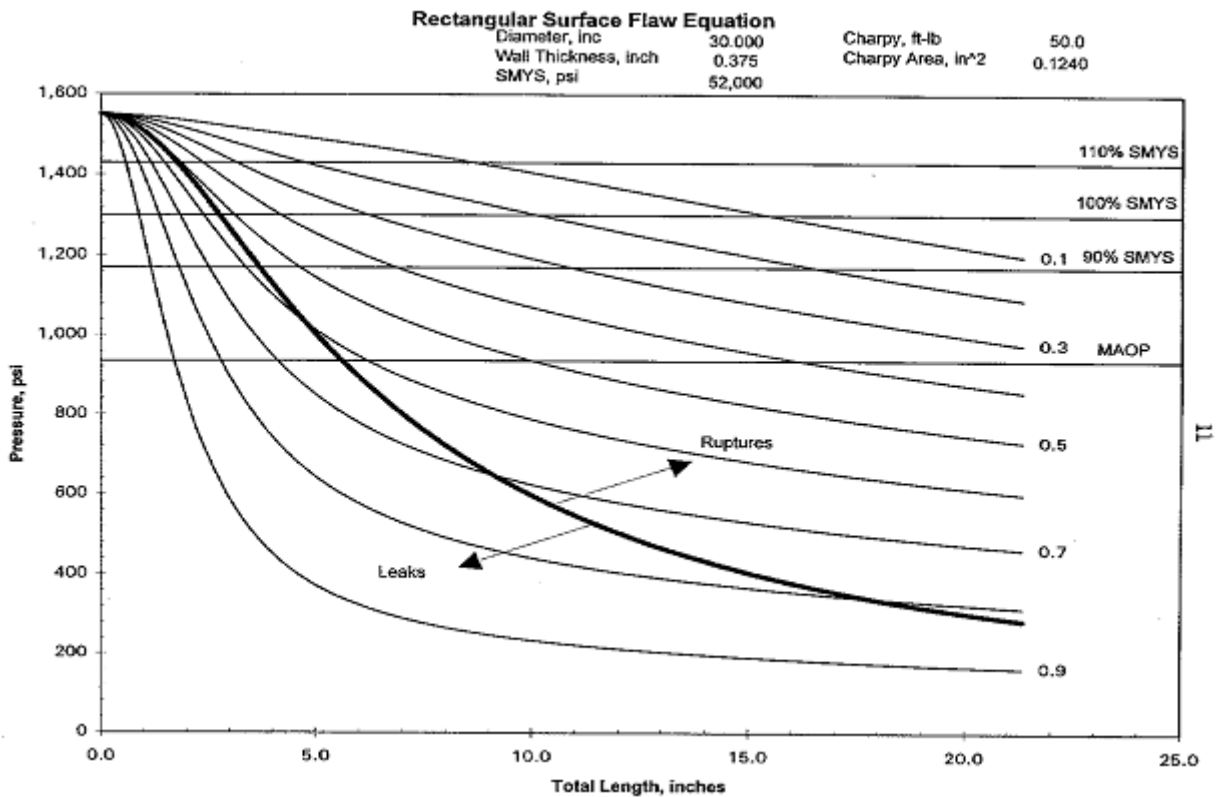
The NTSB metallurgical studies on the pipe sections removed from the San Bruno Incident site (Materials Laboratory Factual Report No. 10-119, National Transportation Safety Board, Washington, DC, January 21, 2011; Materials Laboratory Factual Report No. 11-005, National Transportation Safety Board, Washington, DC, February 9, 2011) provided clear evidence that an initial manufacturing defect was a significant contributor to the eventual failure. The failed piping segment (PUP 1) contained a longitudinal seam weld defect that appeared to extend the full length of that segment – approximately 44 inches – and extended at the worst location some 50 to 55% through the pipe wall from the inner surface. The failed piping segment had been operating at or near its Maximum Allowable Operating Pressure (MAOP) with that defect in place (the amount of defect growth from pressure cycling, either from relatively small pressure

fluctuations of 50 psi or so to full start-up/shut-down pressure cycling is small) for over 50 years, without any apparent manifestations of leakage. This successful operating history – albeit without any initial or in-service hydrostatic pressure testing demonstration of piping structural integrity – offers some evidence that such a defect was not sufficiently deep to be unstable, depending upon the assumed fracture toughness of the weld metal or heat-affected zone material.

In order to assess the stability of this initial manufacturing defect, Figure F4 (see below) from the paper by Kiefner and Maxey (The Benefits and Limitations of Hydrostatic Testing, by John F. Kiefner and Willard A. Maxey) is used for an initial evaluation. Note the graph has been prepared for a 30-inch-diameter, 0.375-inch-thick-walled pipe, with a yield strength of 52,000 psi and a Charpy impact energy of 50 ft-lb. Note also both the yield strength and the Charpy impact energy are far too high for the PUP 1 segment. Using these unrealistically high values, the figure shows that, for an operating pressure of 400 psi, even with a defect 50 to 55% across the wall and infinitely long, no leakage or rupture will occur.

Even with more realistic material property assumptions, an infinitely-long axial defect on the inner surface of the pipe that extends of the order of 50% across the wall can be shown to be stable. With an approximation to the Mode I fracture toughness established at around 45 ksi $\sqrt{\text{in}}$, or even slightly lower for weld metal and heat-affected zone material, that stability can be demonstrated, by using the stress intensity factor solutions in Annex C of API 579 (API 579-1/ASME FFS-1, Fitness-For-Service, Second Edition, American Petroleum Institute, July 2007), with an internal pressure of 400 psi. For an infinitely-long 40% through-wall defect, the applied stress intensity was calculated to be about 22 ksi $\sqrt{\text{in}}$; for an infinitely-long, 60% through-wall defect, the applied stress intensity was calculated to be about 50 ksi $\sqrt{\text{in}}$. In other words, for an infinitely-long internal surface defect, instability would be expected with a defect depth of the order of 60% of the wall thickness. Therefore, an initial longitudinal seam weld defect in PUP 1 that extended the full length of that piping segment (about 44 inches) and which extended through the wall on the order of 50 to 55% would have been marginally stable and have survived fifty or more years of service operating at MAOP.

Figure F4: Impact of Test Pressure Levels on Margin of Safety



Initial Manufacturing Defect Growth Assessment

The next logical question is: How does defects that has remained stable for so many years of operation at or near MAOP grow to critical dimensions? To answer this question, note growth rates of cracks in pipeline steels depend significantly on two parameters – the range of the applied stress intensity at the tip of the crack, called ΔK , and the ratio of the minimum applied stress intensity to the maximum applied stress intensity, called the R ratio or K_{min}/K_{max} . For the case of defect growth during a cycle of pressurization to MAOP, complete depressurization, and pressurization back to MAOP, the applied stress intensity range is relatively large; however, $R = 0$. For the case of defect growth during a pressure fluctuation of 10% of MAOP, the applied stress intensity range is relatively small; however, R could be close to unity.

To compare defect growth rates, the procedure used by Kiefner and Rosenfeld (“Effects of Pressure Cycles on Gas Pipelines,” by John F. Kiefner and Michael J. Rosenfeld, Report No. GRI-04/0178, Gas Research Institute, Des Plaines, IL, September 17, 2004), can be followed. Kiefner and Rosenfeld used the Paris crack growth law constants from API 579. Using two different sets of cycles – a pressurization-depressurization-re-pressurization cycle every year with a stress intensity range of 35 ksi \sqrt{in} and a daily pressure fluctuation with a conservative

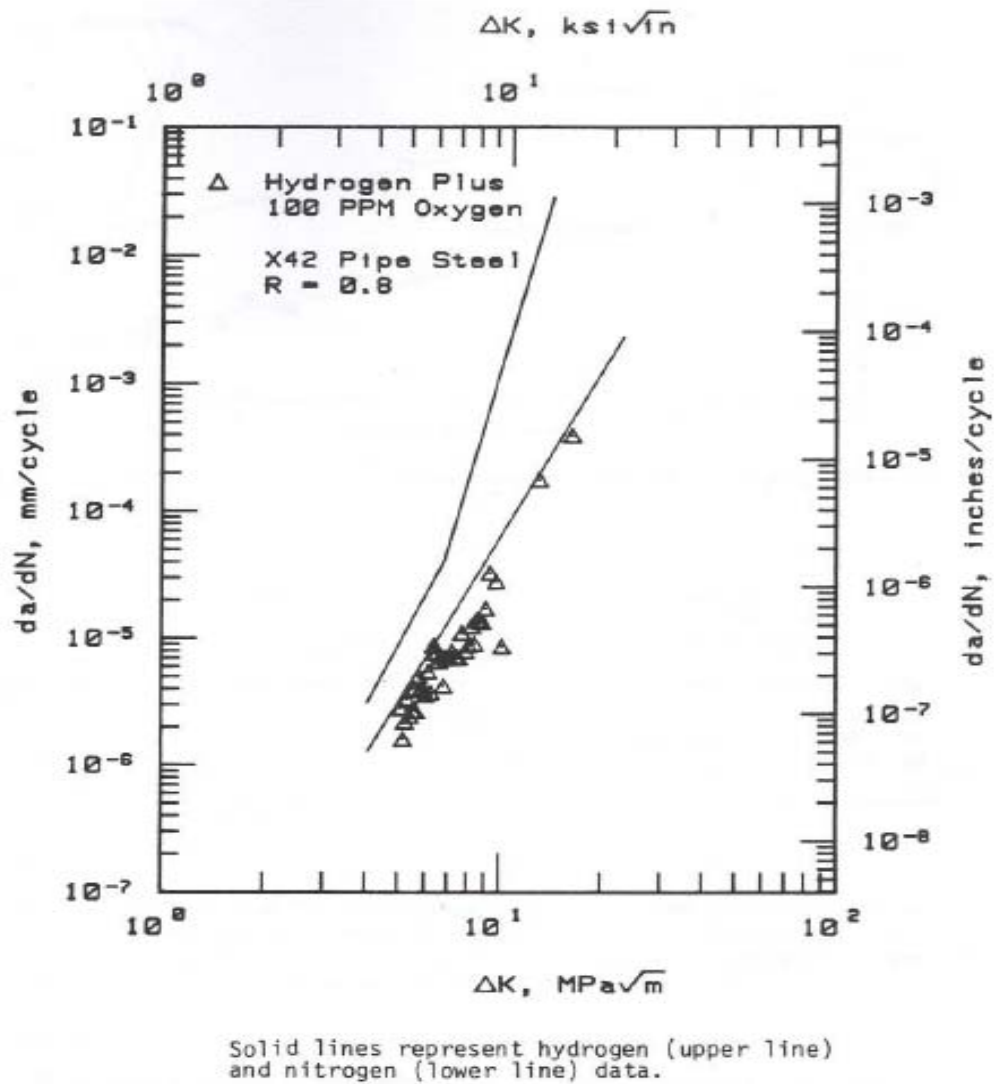
stress intensity range of $7 \text{ ksi}\sqrt{\text{in}}$ – the total amount of defect growth over a 60-year period would be less than 0.01 inches. This growth would increase the depth of the original manufacturing defect from 55% of the wall thickness to no more than 57.5% of the wall thickness.

However, the Paris crack growth law constants used by Kiefner and Rosenfeld did not take the R ratio into account. Typically, the Paris crack growth constants are obtained from fully-reversed crack growth testing ($R = -1$). When $R = 0$, the crack growth rates are of the order of twice those for $R = -1$. For R ratios approaching unity, the crack growth rates are of the order of three times the crack growth rates for $R = -1$. Based on the figure below – taken from the paper “Assessing the Durability and Integrity of Natural Gas Infrastructures for Transporting and Distributing Mixtures of Hydrogen and Natural Gas,” by I. Alliat and J. Heerings – crack growth data for X42 pipeline steel that is exposed to a benign nitrogen environment can be examined (the lower curve), with crack growth rates based on $R = 0.8$ (the crack tip is under moderately high tensile stress throughout the loading cycle).

In this case, for ΔK of $35 \text{ ksi}\sqrt{\text{in}}$ (a full pressurization and complete depressurization cycle), the amount of defect growth for one cycle per year and 60 years of operation would be about 0.006 inches. For ΔK of $7 \text{ ksi}\sqrt{\text{in}}$, the growth for a daily cycle for 60 years would be about 0.018 inches. The combination of cycles could take a defect that is 55% through wall (0.206 inches deep in a 0.375-inch-thick wall) to a defect that is still less than 65% through wall.

Therefore, even assuming annual start-up/shut-down cycles and thousands or hundreds of thousands of modest pressure fluctuation cycles, the amount of stable propagation of the initial defect in the radial direction could possibly lead to a critical and unstable defect in PUP 1 only if the fracture toughness in the longitudinal seam weld and its heat-affected zone were of the order of $35 \text{ ksi}\sqrt{\text{in}}$. Such a scenario is certainly plausible, but no clear evidence of such growth is available from the NTSB metallurgical evidence.

Figure F5



Alternative Piping Integrity Threats

Although failure from the presence of the initial manufacturing defect and its radial growth during cyclic pressure service is plausible, the possibility of failure from a combination of the initial fabrication defect and some other loading event or events seems to be a more likely scenario. In order to determine the most likely combination of threats, the historical record of natural gas transmission pipeline failures is a potential source of information. For example, the Pipeline Research Committee of the American Gas Association conducted a study of natural gas pipeline incidents that were required to be reported to U. S. federal authorities during the period

from 1985 to 1994² provides some evidence into the range of failure root causes and underlying contributing factors.

The most common cause (32.7%) was external force due to encroachment, which encompasses damage such as dents and gouges from third-party actions, or pipeline operator and contractor activities, and intentional malicious attack. The second most common cause (23.5%) is either internal or external corrosion; with such causes as external weather force (10.2%), which encompasses earth movement such as landslides, heavy rains and floods, and extremely cold temperatures; operator error (6.5%); equipment malfunction (5.2%); and defective welds (4.1%) and defective pipe (3.6%) provide much of the balance. Unattributed causes, or other (10.4%), complete the list.

This failure cause distribution is generally consistent with the Pipeline and Hazardous Materials Safety Administration (PHMSA) classification of both serious (causing at least one fatality) and significant (causing at least \$50,000 in property damage) gas transmission pipeline incidents during the period from 1991 to 2010. For example, of the 132 serious incidents during this period, excavation damage was the cause of 43 incidents (32.5%), the largest grouping. Corrosion (22.8%) was the largest grouping among the 1,139 significant incidents, with material/weld/equipment failure (21.0%) a close second and excavation damage (18.3%) third.

These causes and a number of others are listed among the 22 different pipeline integrity threats that are provided as guidance in ASME B31.8S³. ASME B31.8S defines these threats in three categories:

- Time-dependent threats, such as loss of material from internal or external corrosion, and progressive stress corrosion cracking (SCC).
- Time-independent threats, such as third-party mechanical damage, incorrect operational procedures, weather-related phenomena, and earth movements.
- Stable⁴ threats, which include a manufacturing-related defect (e.g., a defective longitudinal weld seam defect) or a fabrication-related defect (e.g., a defective pipe girth weld).

² Patrick H. Vieth, "Analysis of DOT Reportable Incidents," Ninth Symposium on Line Pipe Research, Paper 2, Houston, Texas, September 30-October 2, 1996.

³ Managing System Integrity of Gas Pipelines, ASME B31.8S, American Society of Mechanical Engineers, New York, NY, 2010.

⁴ The term "stable" is somewhat problematical since, while a manufacturing-related or fabrication-related defect may not be explicitly dependent on time, the sub-critical defect growth to potential instability may be implicitly cyclic loading time dependent.

All of these threats and combinations of threats are to be addressed by the gas transmission pipeline operator's Integrity Management Program (IMP).

One immediate observation from this list of threats is the prevalence of third-party risk as a historical contributor to gas transmission pipeline failure; however, the presence of a manufacturing or fabrication defect at the same time raises serious questions about the potential for threat interaction and the subsequent total risk quantification. For example, does the current *additive* approach to risk quantification in the PG&E IMP adequately take into account the potential for *multiplicative* threat interaction? A simple example to consider would be the potential for soil movement that might cause longitudinal seam weld defect growth. A second observation, based on the activity accompanying the June 2008 sewer replacement project, is the propensity for third-party risk to be characterized entirely by *direct* contact with the piping, as opposed to effects that might be caused by *proximity without direct contact*, such as causing excessive lateral or vertical deflection of the piping by incorrect back-filling procedures or by vibratory effects on soil movement and support.

As a point of discussion of this effect, in the NTSB metallurgical Report No. 10-119, the longitudinal weld seam on the relatively long run south of PUP 1 is readily visible and would have been readily visible during the excavation for the sewer replacement project. That particular longitudinal seam was located near the top of the pipe segment (see Table 1), while the longitudinal weld seam for PUP 1, which probably would not have been visible, was located at about 70° from the top of the pipe on the east side of the piping run. NTSB Report No. 10-119 fixed the initiation point for the failure at the PUP 1 longitudinal seam roughly half way between the connections to the south end long run and PUP 2 (see Figures 33a and 33b from NTSB Report No. 10-119, shown below in Figure F6).

Figure F6

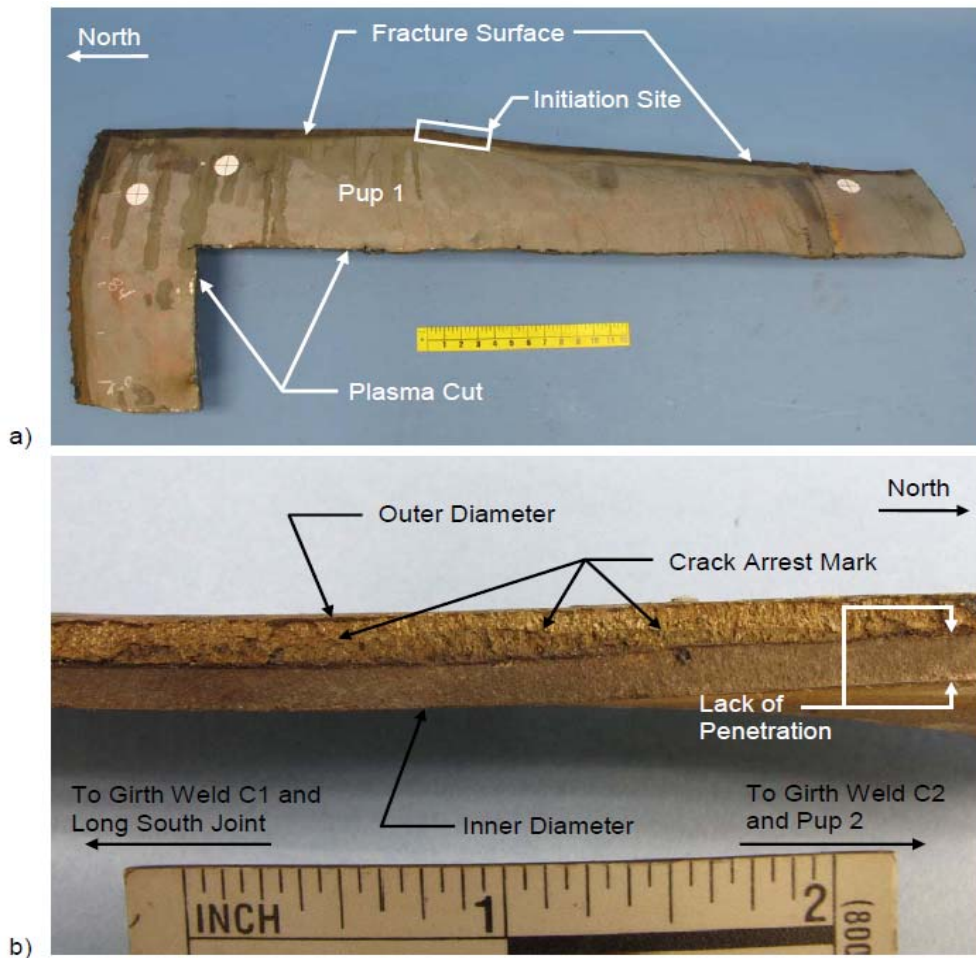


Figure 33: a) Counterclockwise half of pup 1 longitudinal fracture with the location of the crack initiation site indicated; b) cross section view of the longitudinal seam at the initiation site.

Note Figure 33b of the longitudinal weld cross section at the initiation site shows the initial 50 to 55% lack of weld penetration through-wall defect, with no clear evidence of cyclic crack growth extension of that defect. Also shown in the figure, without much explanation, are what are referred to as fairly localized “crack arrest marks” near the initiation site. These marks could be interpreted as stable extension of the initial defect, caused by a single event, out to somewhere in the neighborhood of 75 to 80% of the wall thickness.

If some type of localized effect, such as localized soil pressure or inadvertent third-party action, caused that additional defect growth, that growth would likely take place over a much shorter distance than the full 44-inch length of PUP 1. In order to investigate this possibility, an additional set of stress intensity factor solutions in Annex C of API 579 was evaluated for a finite-length longitudinal defect on the internal surface of a pipe under internal pressure (see Section C.5.10 of API 579). Only one such solution is discussed here – the case of a defect

that has grown from around 55 to 60% through wall to 80% through wall in a local portion of the incomplete PUP 1 weld.

Four different defect lengths were evaluated – 2.4 inches long, 4.8 inches long, 9.6 inches long, and 19.2 inches long. In all cases the driving pressure was assumed to be 400 psi. The evaluations showed that, for the 2.4 inch long defect, the applied stress intensity was only about 25 ksi $\sqrt{\text{in}}$, implying that such a short defect –although very deep – would not be unstable. For the 4.8 inch long defect, the applied stress intensity factor was about 36 ksi $\sqrt{\text{in}}$, which implies marginal but likely defect stability. Both the 9.6 inch long and 19.2 inch long defects were unstable.

Therefore, it would appear that localized acceleration of growth from the original manufacturing welding defect is an alternative and more likely failure scenario. At present, such localized growth must be considered anomalous absent some evidence of localized soil movement, or some phenomenon that locally increased soil pressure, or a third-party action that could have led to localized bending or ovalization of the pipe in the region near PUP 1. Localized bending or ovalization would be of particular concern if the stresses on the interior of the pipe caused by denting or ovalization were locally tensile at the azimuthal position of the longitudinal weld, adding to the circumferential pressure tensile stresses.)

NTSB Findings to Date

The NTSB investigation has not yet determined the root cause and any underlying contributing factors that led to the San Bruno pipeline failure, and will not issue its report on the incident for several months. However, the NTSB has recognized the failed San Bruno pipe section contained a longitudinal seam weld with a defect that extended the full length of PUP 1 and about 50 to 55% across the pipe wall. Because of this recognition, the NTSB recommended PG&E and other natural gas transmission pipeline operators should review their records to assure: (1) the mischaracterization by PG&E of the San Bruno pipe segment as seamless is not a systemic error, (2) any longitudinal seam-welded piping is properly characterized and appropriately classified in terms of risk, and (3) the risk associated with similar defects in other piping segments is appropriately mitigated.

The NTSB interim findings to date are both reasonable and useful, especially with respect to:

- Discovery that the failed piping was of longitudinal-seam-welded construction, rather than seamless.
- Discovery that the failed piping was composed of several short, girth-weld-connected segments.
- Identification of record keeping deficiencies by PG&E related to pipe characterization and MAOP determination.

- Production of useful metallurgical information on the failed piping, including relatively low Charpy V-notch energies for the base metal and some relatively low yield and ultimate strength values for some of the PUP segments.

All four of these interim findings raised significant issues with respect to legacy gas transmission piping in general and with respect to PG&E's legacy gas transmission piping, in particular. For PG&E, the unavailability of at least some legacy piping records and potential mischaracterization of other legacy piping records raised the issue of whether threats similar to the Line 132 San Bruno segment are currently unidentified.

Those legacy piping segments for which PG&E was unable to retrieve adequate documentation to confirm the piping characteristics are expected to undergo hydrostatic pressure testing over the next several months, with the test pressure planned to be 150% of the Maximum Allowable Operating Pressure (MAOP). The purpose of the relatively high test pressure is not only to expose any defects that threaten future operation at MAOP, but also to drive even smaller defects to instability (leakage or rupture), potentially generating a greater degree of integrity demonstration. The defects that threaten future operation are those that have been and are currently *stable*, but which have margins of safety that have been reduced to the point that uncertainties in material behavior, loadings, or environments could cause *instability*.

Hydrostatic pressure testing of uncharacterized legacy piping with potentially low fracture toughness may not be the optimum approach, depending upon whether the San Bruno Incident is viewed as an anomaly that is not likely to exist elsewhere in the PG&E transmission system, or whether the San Bruno Incident is viewed as evidence of potentially more systemic behavior. If systemic issues are suspected, another option is available that would either be a precursor to hydrostatic pressure testing, or which would replace some or even most of the hydrostatic pressure testing. That option would involve excavating and exposing any longitudinal seam welds along segments of uncharacterized legacy piping, probably at a frequency of every mile or every other mile, while using a tool such as the automated ball indenter to characterize the piping material. Such testing would include indenter determination of yield strength and "indentation energy to fracture," but could also entail a circumferential hardness traverse to locate the longitudinal seam weld and its heat-affected zones, with the potential for a volumetric non-destructive examination (e.g., ultrasonic testing) to determine any significant defect structure on the interior of the pipe. Destructive examination to remove an occasional section of the pipe (which would involve shutting down an occasional transmission line segment) to measure Charpy impact energy for confirmation of automated ball indenter results could be considered.